International Journal of Numerical Methods for Heat & Fluid Flow

Entropy generation optimization for MHD natural convection of a nanofluid in porous media-filled enclosure with active parts and viscous dissipation

M.A. Mansour Sameh Elsayed Ahmed Ali J. Chamkha

Entropy generation optimization for MHD natural convection of a nanofluid in porous media-filled enclosure with active parts and viscous dissipation

Received 9 October 2015
Revised 29 December 2015
Accepted 4 January 2016

M.A. Mansour
Department of Mathematics, Assuit University, Faculty of Science, Assuit, Egypt
Sameh Elsayed Ahmed
Department of Mathematics, South Valley University, Qena, Egypt, and
Ali J. Chamkha
Department of Mechanical Engineering, Prince Mohammad Bin Fahd University, Al-Khobar, Saudi Arabia

Abstract

Purpose – This paper aims to investigate the entropy generation due to magnetohydrodynamic natural convection flow and heat transfer in a porous enclosure filled with Cu-water nanofluid in the presence of viscous dissipation effect. The left and right walls of the cavity are thermally insulated. There are heated and cold parts, and these are placed on the bottom and top wall, respectively, whereas the remaining parts are thermally insulated.

Design/methodology/approach – The finite volume method is used to solve the dimensionless partial differential equations governing the problem. A comparison with previously published woks is presented and is found to be in an excellent agreement.

Findings – The minimization of entropy generation and local heat transfer according to different values of the governing parameters are presented in details. It is found that the presence of magnetic field has negative effects on the local entropy generation because of heat transfer and the local total entropy generation. Also, the increase in the heated part length leads to a decrease in the local Nusselt number.

Originality/value – This problem is original, as it has not been considered previously.

Keywords Viscous dissipation, MHD, Nanofluid, Porous media, Entropy generation, Cavity with active parts

Paper type Research paper

Nomenclatures

B	= dimensionless heat source length
b	= dimensional heat source length
Be	= Bejan number
C_p	= heat capacitance
D	= dimensionless heat source location
d	= dimensional heat source location
Da	= Darcy number

International Journal of Numerical Methods for Heat & Fluid Flow
Vol. 27 No. 2, 2017
pp. 379-399

0961-5539
DOI 10.1108/HFF-10-2015-0408

g = gravity acceleration
H = height of the cavity
Ha = Hartmann number
K = permeability of the porous medium
k = thermal conductivity
Nu = Nusselt number
Nu_m = average Nusselt number
p = dimensional pressure
P = dimensionless pressure
Pr = Prandtl number
Ra = Rayleigh number
S_0 = characteristic entropy generation rate
S_{tot} = local total entropy generation
T = dimensional temperature
T_o = reference temperature
(u, v) = dimensional velocity component
(U, V) = dimensionless velocity component
(x, y) = dimensional Cartesian coordinates
(X, Y) = dimensionless Cartesian coordinates

Greek symbols

α = thermal diffusivity
β = thermal expansion
β_0 = magnetic field strength
θ = dimensionless temperature
Θ = irreversibility ratio
ρ = density
σ = electrical conductivity
υ = kinematic viscosity
μ = dynamic viscosity
φ = solid volume fraction
ε = viscous dissipation parameter

Subscripts

c = cold
f = fluid
h = hot
nf = nanofluid
p = solid particles
w = wall

1. Introduction

Many researchers were interested in studying the natural convective heat transfer in a fluid-saturated porous media because of its importance in many applications in thermal insulation systems, geothermal engineering, porous heat exchangers, food storage, underground disposal of nuclear waste materials, oil separation from sand by steam, electronic device cooling, etc. Vafai (2005), Nield and Bejan (2006) and Ingham and Pop (2002) presented representative reviews of these applications and other heat transfer applications in porous media. Additionally, there are many published studies related to natural convection

in rectangular porous enclosures. Moya *et al.* (1987), Bejan (1979), Parsad and Kulacki (1984), Baytas and Pop (1999), Beckermann *et al.* (1986), Gross *et al.* (1986), Lai and Kulacki (1988), Manole and Lage (1992) and Walker and Homsy (1978) have donated many important results for this problem.

The problem of entropy generation due to natural convection and heat transfer in an inclined porous medium-filled cavity using Darcy's law and Boussinesq incompressible approximation were investigated by Baytas (2000). Shohel and Roydon (2002) studied the problem of magnetohydrodynamic (MHD) mixed convection through a vertical channel in the presence of thermal radiation effects. Special focus is given on the entropy generation characteristics and its dependency on various dimensionless parameters. Shohel and Sadrul (2003) used the finite element method to solve the dimensionless equations governing the heat transfer and fluid flow characteristics in a wavy enclosure.

Saeid (2006) investigated the natural convection cooling of two heated elements located on adiabatic vertical plate immersed in a Darcian porous medium. His results show that the increase in any of the governing parameter results in an enhancement in the average Nusselt number along the upper element. Varol *et al.* (2008) used the support vector machine technique to discusses the fluid flow and temperature distributions in a square porous enclosure that contains three heaters embedded in the left vertical wall. Kaluri and Basak (2011) investigated the optimal configuration for natural convection in a porous square enclosure with discrete flush-mounted heat sources arranged in different configurations using entropy generation minimization approach. The distributed heating methodology with multiple heaters is found to be an efficient strategy for thermal mixing, temperature uniformity and minimum entropy generation. Soleimani *et al.* (2011) studied the location of wall-mounted heat source and sink arranged in a parallel manner and found optimized configuration as a function of Rayleigh number (Ra) and size of source and sink.

MHD natural convection flow associated with heat transfer has received considerable attention in the recent years because of its wide variety of application in engineering areas, such as crystal growth in liquid, cooling of nuclear reactor, electronic package, microelectronic devices and solar technology. Kandaswamy *et al.* (2008) studied the MHD natural convection of an electrically conducting fluid in a square cavity with thermally active vertical wall. The results show that the rate of heat transfer takes its maximum at the center of the active parts, whereas it is poor for the top–bottom thermally active locations. Also, an increase in the Hartmann number leads to reduce the average Nusselt number. The problem of MHD natural convection flow and heat of an electrically conducting fluid inside an inclined cavity with heated bottom wall and cooled top wall was investigated by Pirmohammadi and Ghassemi (2009). Their results show that at $Ra = 10^5$, the Nusselt number increases up to about $\varphi = 45°$ and then decreases as φ increases. Grosan *et al.* (2009) have studied the effects of the magnetic field and internal heat generation on the free convection in a rectangular cavity filled with a porous medium. With the growing demand for efficient cooling systems, particularly in the electronics industry, more effective coolants are required to keep the temperature of electronic components below safe limits so that the heat transfer enhancement in engineering is one of the hottest topics in research. A good survey for the presented study can be found in papers by Cho (1995), Xuan and Li (2000), Khanafer *et al.* (2003), Mahmoudi *et al.* (2010), Oztop and Abu-Nada (2008), Aminossadati and Ghasemi (2011), Talebi *et al.* (2010), Mahmoodi and Hashemi (2012), Sun and Pop (2011), Farooji *et al.* (2012), Abu-Nada (2011), Abu-Nada *et al.* (2010), Sebdani *et al.* (2012), Hamad (2011), Ghasemi *et al.* (2011), Nemati *et al.* (2012), Hamad and Pop (2011), Aminossadati *et al.* (2011) and Mahmoudi *et al.* (2013).

For nanofluid flow over different shapes, Noghrehabadi *et al.* (2012, 2013a, 2013b and 2013c) present representative reviews for this topic. Noghrehabadi *et al.* (2012) studied the slip effects on the boundary layer flow and heat transfer over a stretching surface in the presence of nanoparticle fractions. Their results showed that the flow velocity and the surface shear stress on the stretching sheet are strongly influenced by the slip parameter. The problem of boundary layer heat transfer and entropy generation of a nanofluid over an isothermal linear stretching sheet with heat generation/absorption was investigated by Noghrehabadi *et al.* (2013a). They found that an increase in heat generation parameter, Brownian motion parameter or thermophoresis parameter decreases the entropy generation number in the vicinity of the sheet. Noghrehabadi *et al.* (2013b) discussed the non-Darcy flow and natural convection over a vertical cone embedded in a porous medium saturated with a nanofluid and studied it using the Forchheimer-extended Darcy law. They observed that an increase in the non-Darcy parameter would decrease the reduced Nusselt and Sherwood numbers, whereas an increase in the Lewis number would increase the reduced Nusselt and Sherwood numbers. The natural convection heat and mass transfer of nanofluids over a vertical plate embedded in a saturated Darcy porous medium subjected to surface heat and nanoparticle fluxes was investigated by Noghrehabadi *et al.* (2013c). Their results indicated that an increase in the Lewis number increases both the reduced Nusselt number and the Sherwood number.

Motivated by the investigations mentioned above, the main objective of the current investigation is to study the effects of a horizontal magnetic field and viscous dissipation on the entropy generation due to steady natural convection flow of an electrically conducting nanofluid in a square enclosure filled with isotropic porous medium with active horizontal walls. The Darcy model and Boussinesq incompressible approximation are used to formulate the governing equations of the problem. The results of the problem are presented in terms of streamlines, isotherms, entropy generation due to heat transfer and total entropy generation, as well as average total entropy generation, average Bejan number and profiles of the local Nusselt number along the heat source.

2. Mathematical modeling

MHD natural convective flow of a nanofluid in the presence of viscous dissipation inside a square enclosure of width and height (H) filled with fluid-saturated porous medium is considered in the present work. The schematic diagram is displayed in Figure 1. In the present simulation, the following assumptions have been made:

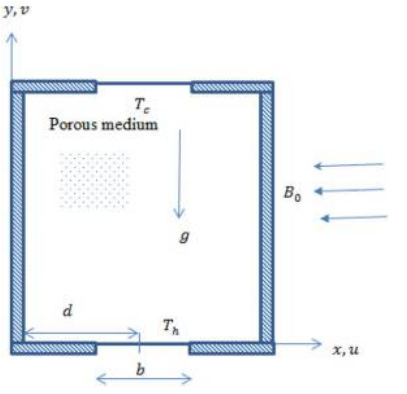

Figure 1.
Physical model of the problem

- In the cavity, the left and right walls are thermally insulated.
- A heat source is located on a part of the bottom wall and the other parts are thermally insulated.
- A part of the top wall of the cavity is maintained at T_c such that $T_h > T_c$, whereas the other parts are thermally insulated.
- The gravity acts in the vertical direction. Also, thermo-physical properties for the base fluid and the nanoparticles are shown in Table I.
- The base fluid (water) and the solid spherical nanoparticles are in thermal equilibrium.
- The Boussinesq approximation is used to determine the variation of density in the buoyancy term where the other thermo-physical properties of the nanofluid are assumed constant.
- The porous medium is considered to be a homogeneous and isotropic. Also, the local thermal equilibrium model between the nanofluid and porous matrix is applicable.

Under these assumptions, the continuity, momentum, energy and entropy generation equations can be expressed as (Al-Hadhrami *et al.*, 2003):

$$\frac{\partial u}{\partial x} + \frac{\partial v}{\partial y} = 0, \tag{1}$$

$$u\frac{\partial u}{\partial x} + v\frac{\partial u}{\partial y} = -\frac{1}{\rho_{nf}}\frac{\partial p}{\partial x} + \nu_{nf}\left(\frac{\partial^2 u}{\partial x^2} + \frac{\partial^2 u}{\partial y^2}\right) - \frac{\nu_{nf}}{K}u - \frac{\sigma_{nf}B_0^2}{\rho_{nf}}u, \tag{2}$$

$$u\frac{\partial v}{\partial x} + v\frac{\partial v}{\partial y} = -\frac{1}{\rho_{nf}}\frac{\partial p}{\partial y} + \nu_{nf}\left(\frac{\partial^2 v}{\partial x^2} + \frac{\partial^2 v}{\partial y^2}\right) - \frac{\nu_{nf}}{K}v + \frac{(\rho\beta)_{nf}}{\rho_{nf}}g(T - T_0), \tag{3}$$

$$u\frac{\partial T}{\partial x} + v\frac{\partial T}{\partial x} = \alpha_{nf}\left(\frac{\partial^2 T}{\partial x^2} + \frac{\partial^2 T}{\partial y^2}\right) + \frac{\mu_{nf}}{(\rho c_p)_{nf}}\left\{\frac{1}{K}(u^2 + v^2) + 2\left[\left(\frac{\partial u}{\partial x}\right)^2 + \left(\frac{\partial v}{\partial y}\right)^2\right] + \left(\frac{\partial u}{\partial y} + \frac{\partial v}{\partial x}\right)^2\right\}, \tag{4}$$

$$S_{gen} = \left(\frac{k_{nf}}{T_0^2}\right)\left[\left(\frac{\partial T}{\partial x}\right)^2 + \left(\frac{\partial T}{\partial y}\right)^2\right] + \left(\frac{\mu_{nf}}{T_0}\right)\left\{\frac{1}{K}(u^2 + v^2) + 2\left[\left(\frac{\partial u}{\partial x}\right)^2 + \left(\frac{\partial v}{\partial y}\right)^2\right] + \left(\frac{\partial u}{\partial y} + \frac{\partial v}{\partial x}\right)^2\right\} + \left(\frac{\sigma_{nf}}{T_0}\right)B_0^2 u^2. \tag{5}$$

Property	Water	Cu
ρ	997.1	8,933
C_p	4,179	385
k	0.613	401
β	21×10^{-5}	1.67×10^{-5}
σ	0.05	5.96×10^7

Source: Aminossadati and Ghasemi (2011)

Table I. Thermo-physical properties for the base fluid and the nanoparticles

In equations (1)-(5), x and y are Cartesian coordinates measured along the horizontal and vertical walls of the cavity respectively, u and v are the velocity components along the x- and y- axes respectively, T is the fluid temperature, p is the fluid pressure, g is the gravity acceleration, K is the permeability and $T_0 = (T_h + T_c)/2$ is the reference temperature.

Numerous formulations for the thermo-physical properties of nanofluids are proposed in the literature (Khanafer *et al.*, 2003). In the present study, we are adopting the relations which depend on the nanoparticles' volume fraction only and which were proven and used in many previous studies Einstein (1956) and Brinkman (1952) as follows:

The effective density of the nanofluid is given as:

$$\rho_{nf} = (1 - \varphi)\rho_f + \varphi\rho_p, \tag{6}$$

where φ is the solid volume fraction of the nanofluid, ρ_f and ρ_p are the densities of the fluid and solid fractions, respectively, and the heat capacitance of the nanofluid given is by Khanafer *et al.* (2003) as:

$$(\rho c_p)_{nf} = (1 - \varphi)(\rho c_p)_f + \varphi(\rho c_p)_p. \tag{7}$$

The thermal expansion coefficient of the nanofluid can be determined by:

$$(\rho\beta)_{nf} = (1 - \varphi)(\rho\beta)_f + \varphi(\rho\beta)_p. \tag{8}$$

where β_f and β_p are the coefficients of thermal expansion of the fluid and solid fractions, respectively.

Thermal diffusivity, α_{nf} of the nanofluid is defined by Oztop and Abu-Nada (2008) as:

$$\alpha_{nf} = \frac{k_{nf}}{(\rho c_p)_{nf}}. \tag{9}$$

In equation (9), k_{nf} is the thermal conductivity of the nanofluid, which for spherical nanoparticles, according to the Maxwell-Garnetts model (Maxwell, 1904), is:

$$\frac{k_{nf}}{k_f} = \frac{(k_p + 2k_f) - 2\varphi(k_f - k_p)}{(k_p + 2k_f) + \varphi(k_f - kp)}. \tag{10}$$

The effective dynamic viscosity of the nanofluid based on the Brinkman (1952) model is given by:

$$\mu_{nf} = \frac{\mu_f}{(1 - \varphi)^{2.5}}, \tag{11}$$

where μ_f is the viscosity of the fluid fraction, and the effective electrical conductivity of nanofluid was presented by Maxwell (1904) as:

$$\frac{\sigma_{nf}}{\sigma_f} = 1 + \frac{3(\gamma - 1)\varphi}{(\gamma + 2) - (\gamma - 1)\varphi}, \tag{12}$$

where $\gamma = \sigma_p/\sigma_f$

Introducing the following dimensionless set:

$$X = \frac{x}{H},\ Y = \frac{y}{H},\ U = \frac{uH}{\alpha_f},\ V = \frac{vH}{\alpha_f},\ P = \frac{pH^2}{\rho_{nf}\alpha_f^2},\ \theta = \frac{T - T_c}{\Delta T},$$
$$\Delta T = (T_h - T_c),\ D = \frac{d}{H},\ B = \frac{b}{H} \tag{13}$$

and substituting equation (13) in equations (1)-(5), we obtain:

$$\frac{\partial U}{\partial X} + \frac{\partial V}{\partial Y} = 0, \tag{14}$$

$$U\frac{\partial U}{\partial X} + V\frac{\partial U}{\partial Y} = -\frac{\partial P}{\partial X} + \frac{\mu_{nf}}{\rho_{nf}\alpha_f}\left(\frac{\partial^2 U}{\partial X^2} + \frac{\partial^2 U}{\partial Y^2} - \frac{U}{Da}\right) - Ha^2 \cdot \mathrm{Pr} \cdot \frac{\sigma_{nf}}{\sigma_f} \cdot \frac{\rho_f}{\rho_{nf}} U, \tag{15}$$

$$U\frac{\partial V}{\partial X} + V\frac{\partial V}{\partial Y} = -\frac{\partial P}{\partial Y} + \frac{\mu_{nf}}{\rho_{nf}\alpha_f}\left(\frac{\partial^2 V}{\partial X^2} + \frac{\partial^2 V}{\partial Y^2} - \frac{V}{Da}\right) + \frac{(\rho\beta)_{nf}}{\rho_{nf}\beta_f} Ra\mathrm{Pr}\,\theta, \tag{16}$$

$$U\frac{\partial \theta}{\partial X} + V\frac{\partial \theta}{\partial Y} = \frac{\alpha_{nf}}{\alpha_f}\left[\frac{\partial^2 \theta}{\partial X^2} + \frac{\partial^2 \theta}{\partial Y^2}\right] + \frac{1}{(1-\phi)^{2.5}}\frac{1}{\left[1 - \phi + \phi\frac{(\rho C_p)_p}{(\rho C_p)_f}\right]}$$
$$\varepsilon\left[[U^2 + V^2] + 2Da\left[\frac{\partial U}{\partial X}\right]^2 + 2Da\left[\frac{\partial V}{\partial Y}\right]^2 + Da\left[\frac{\partial U}{\partial Y} + \frac{\partial V}{\partial X}\right]^2\right], \tag{17}$$

$$Stot = \frac{S_{gen}}{S_0}$$
$$= \left(\frac{k_{nf}}{k_f}\right)\left[\left(\frac{\partial \theta}{\partial X}\right)^2 + \left(\frac{\partial \theta}{\partial Y}\right)^2\right] + \Theta\left(\frac{\mu_{nf}}{\mu_f}\right)\left\{(U^2 + V^2) + Da\left[2\left(\left(\frac{\partial U}{\partial X}\right)^2 + \left(\frac{\partial V}{\partial Y}\right)^2\right)\right.\right.$$
$$\left.\left. + \left(\frac{\partial V}{\partial X} + \frac{\partial U}{\partial Y}\right)^2\right]\right\} + \left(\frac{\sigma_{nf}}{\sigma_f}\right) \cdot Ha^2 \cdot Da \cdot U^2, \tag{18}$$

where:

$$\mathrm{Pr} = \frac{\nu_f}{\alpha_f},\ Ra = \frac{g\beta_f \Delta T H^3}{\nu_f \alpha_f},\ Da = \frac{K}{H^2},\ Ha = B_0 H\sqrt{\frac{\sigma_f}{\mu_f}},\ \varepsilon = \frac{\mu_f \alpha_f}{K(\rho C_p)_f \Delta T} \tag{19}$$

are, respectively, the Prandtl number, the Rayleigh number, the Darcy number, the Hartman number and viscous dissipation parameter. In addition, $S_0 = k_f(\Delta T/H\,T_0)^2$ is the characteristic entropy generation rate. The corresponding irreversibility distribution ratio (Θ) is defined as:

$$\Theta = \frac{\mu_f T_0}{k_f}\left(\frac{\alpha_f^2}{K(\Delta T)^2}\right). \tag{20}$$

The boundary conditions now take the following form:

$$\begin{aligned} &U = V = \frac{\partial \theta}{\partial X} = 0, \quad 0 \le Y \le 1 \quad on\ walles \quad X = 0, 1 \\ &U = V = 0,\ \theta = 0.5, \quad D - 0.5B \le X \le D + 0.5B, \\ &\frac{\partial \theta}{\partial Y} = 0,\ otherwise \quad on\ wall \quad Y = 0 \\ &U = V = 0, \quad \theta = -0.5, \quad D - 0.5B \le X \le D + 0.5B, \\ &\frac{\partial \theta}{\partial Y} = 0,\ otherwise \quad on\ wall \quad Y = 1 \end{aligned} \qquad (21)$$

The local Nusselt number and the average Nusselt number at the heated part are defined as:

$$Nu = \frac{k_{nf}}{k_f}\left(\frac{\partial \theta}{\partial Y}\right)_{Y=0}, \qquad (22)$$

$$Nu_m = \frac{1}{B}\int_{D-B/2}^{D+B/2} Nu\, dX. \qquad (23)$$

The dimensionless Bejan number (Be) (Bejan, 1996) indicates the strength of the entropy generation due to heat transfer irreversibility:

$$Be = \frac{S_\theta}{S_{tot}}, \qquad (24)$$

where

$$S_\theta = \left(\frac{k_{nf}}{k_f}\right)\left[\left(\frac{\partial \theta}{\partial X}\right)^2 + \left(\frac{\partial \theta}{\partial Y}\right)^2\right].$$

The global total entropy generation (S_{av}) in the field can be obtained by integrating the local total entropy generation (S_{tot}) over the domain Ω Lam and Prakash (2014):

$$S_{av} = \int_\Omega S_{tot}\, d\,\Omega. \qquad (25)$$

The global Bejan number (Be_{av}) is given as:

$$Be_{av} = \frac{\int_\Omega S_\theta\, d\Omega}{\int_\Omega S_{tot}\, d\Omega}. \qquad (26)$$

3. Numerical solution procedure

The numerical solution for the governing equations (14)-(17) with the boundary conditions [equation (21)] is based on the finite volume method with semi-implicit method for pressure-linked equations (SIMPLE) algorithm. It is worth mentioning that collocated, regular and orthogonal grids were used in this implementation. Also, Rhie–Chow

interpolation was used. The algebraic equations resulting from this treatment are solved using alternating direct implicit procedure. The details of the current method are presented in more recent paper of Ahmed (2015). To choose the suitable grid for our calculations, a grid independency study is presented in Table II. This table shows the values of the average Nusselt number against six grids, i.e. 31×31, 41×41, 61×61, 81×81, 101×101 and 121×121. It is found that the 121×121 grid is sufficiently enough to solve the system of equations. The unknown dependent variables were calculated iteratively until the following criteria of convergence was fulfilled:

$$\Sigma_{i,j} \left| \chi_{i,j}^{new} - \chi_{i,j}^{old} \right| \leq 10^{-6}, \tag{27}$$

where χ is the general dependent variable.

Figure 2 shows comparisons of our results with the results reported by Ilis *et al.* (2008). It is observed that there is an excellent agreement between the present results and the results reported by Ilis *et al.* (2008).

4. Results and discussion

In this study, fluid flow and thermal characteristics associated with the natural convection heat transfer in a porous enclosure containing active parts in the horizontal walls are studied. The parameters considered in the present study are length of heat source ($0.2 \leq B \leq 0.8$), heat source location ($0.3 \leq D \leq 0.8$), Hartman number ($0 \leq Ha \leq 100$), Darcy number ($10^{-3} \leq Da \leq 10^{-5}$), nanoparticle volume fraction ($0 \leq \phi \leq 0.1$) and viscous dissipation parameter ($10^{-2} \leq \varepsilon \leq 10^{-4}$). In all the obtained results, the values of Pr and Θ are fixed at 6.8 and 10^{-1}, respectively.

Figure 3 presents the contours of streamlines, isotherms, entropy generation due to heat transfer and total entropy generation for different values of heat source length B at $Ra = 10^5$, $Da = 10^{-3}$, $Ha = 50$, $D = 0.5$, $\varepsilon = 10^{-4}$, $\phi = 0.1$. As the heat sources and sink are located in the middle of the bottom and top walls, symmetric flow and temperature distributions are observed inside the enclosure. The streamlines show four counter-rotating circulating cells for all values of heat source lengths. The buoyant forces generated by the fluid temperature differences cause the fluid to rise in the middle and to descend on the sides of the enclosure. This forming movement of the fluid forms counter-rotating circulation cells within the enclosure. The high values of B lead to decay in the fluid motion and the streamlines are pulled toward corners of the cavity. The isotherms lines take a curve paths at small values of B. Increasing the heat source length causes the isotherm lines to take parallel line paths inside the enclosure. Regarding the contours of entropy generation due to heat transfer, it gathered beside the active parts of the cavity. The increase in B leads to a decrease in the temperature gradients and hence decreases the maximum value of the entropy generation due to heat transfer. Also, the fluid irreversible processes are strong at low values of B. The total entropy generation contours gather beside the horizontal wall, and there are three cells inside the core of the cavity. As B increases, the maximum value of the total entropy generation decreases and the total entropy generation contours show very small areas beside the horizontal wall, and there is no irreversible process is happened inside the core of the

Table II. Grid independency study at $Ra = 10^5, Da = 10^{-3}, Ha = 50, B = 0.2, D = 0.5, \varepsilon = 10^{-4}, \phi = 0.1$

Grid size	31×31	41×41	61×61	81×81	101×101	121×121
N_{u_m}	17.80071	18.28863	18.67062	18.82197	18.90121	18.94838

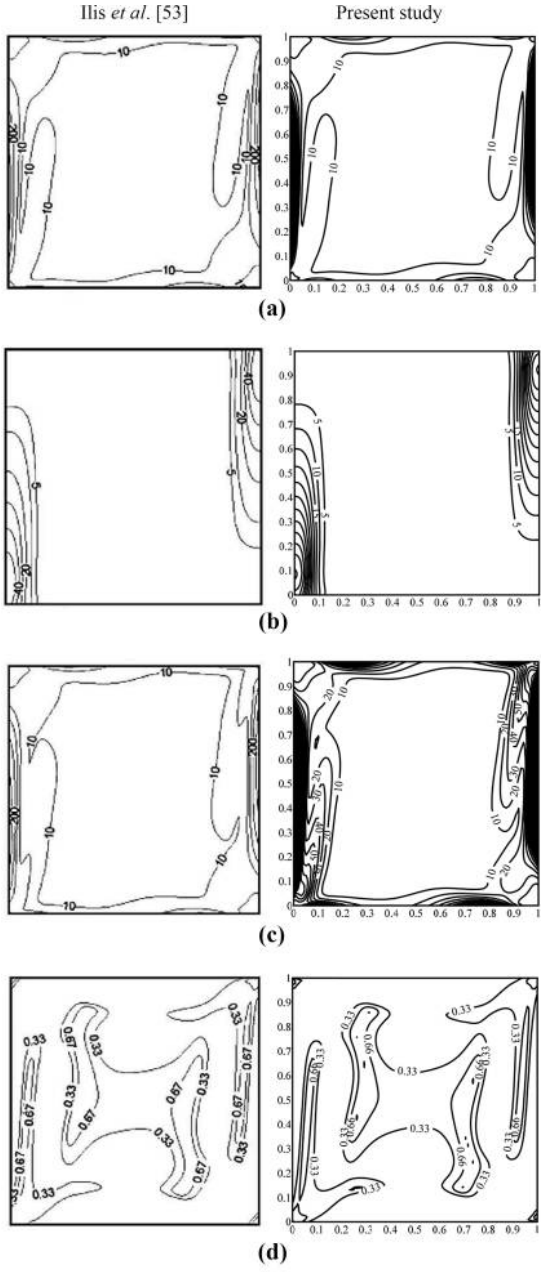

Notes: (a) Fluid friction; (b) local entropy generation due to heat transfer; (c) local total entropy; (d) local Bejan number at $Ra = 10^5$, $\Theta = 10^{-4}$

Figure 2.
Comparison of the present results with reported numerical solutions

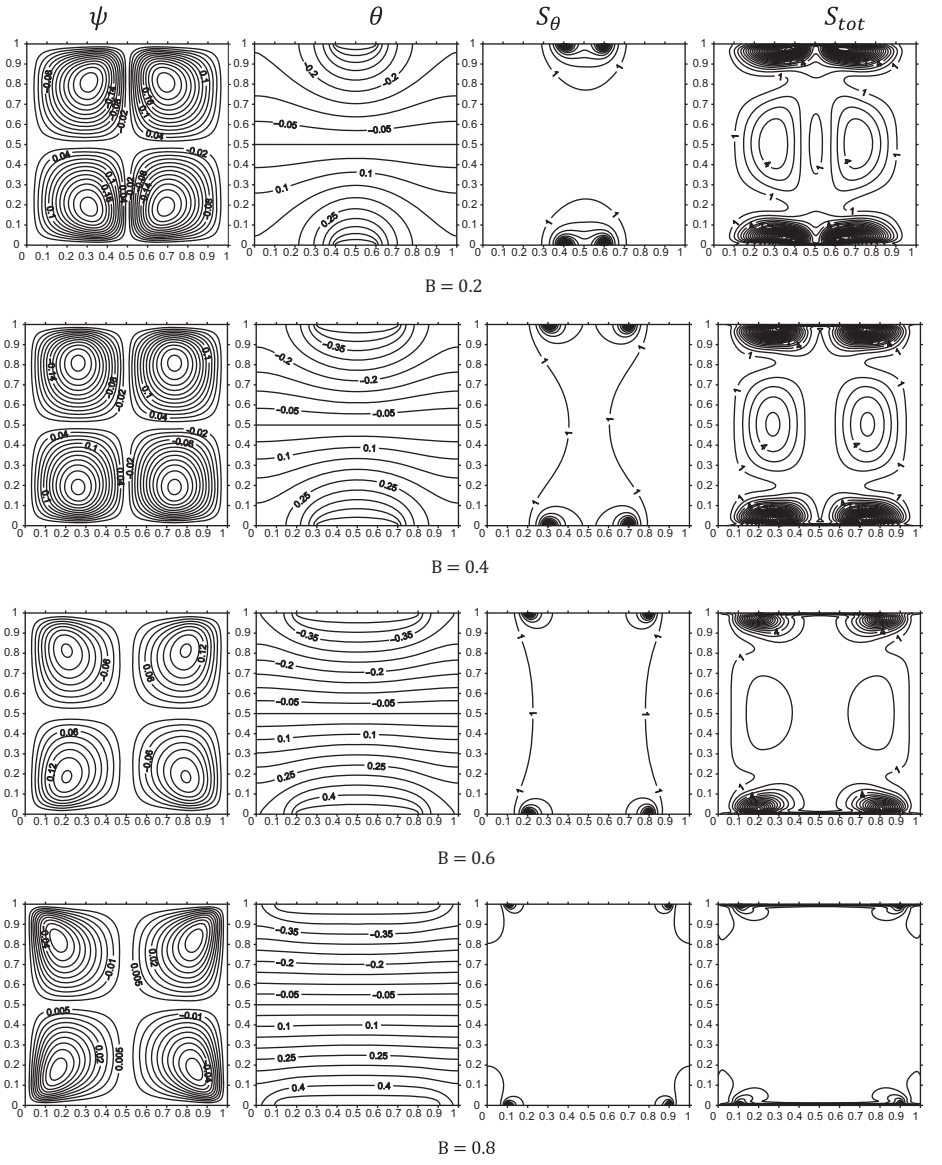

Figure 3. Contours of streamlines, isotherms, entropy generation due to heat transfer and total entropy generation for different values of heat source length B at $Ra = 10^5$, $Da = 10^{-3}$, $Ha = 50$, $D = 0.5$, $\varepsilon = 10^{-4}$, $\phi = 0.1$

cavity. All these observations indicate that a weak convective is obtained by increasing the heat source length. This is due to an increase in the cold part of the top wall by increase B.

Figure 4 shows the contours of streamlines, isotherms, entropy generation due to heat transfer and total entropy generation for different values of Hartmann number Ha at $Ra = 10^5, Da = 10^{-3}, B = 0.2, D = 0.5, \varepsilon = 10^{-4}, \phi = 0.1$. It is observed that for all values of Ha, there are four clockwise and counter clockwise eddies that are formulated inside the cavity. Also, symmetrical temperature distributions are obtained. In the absence of a magnetic force

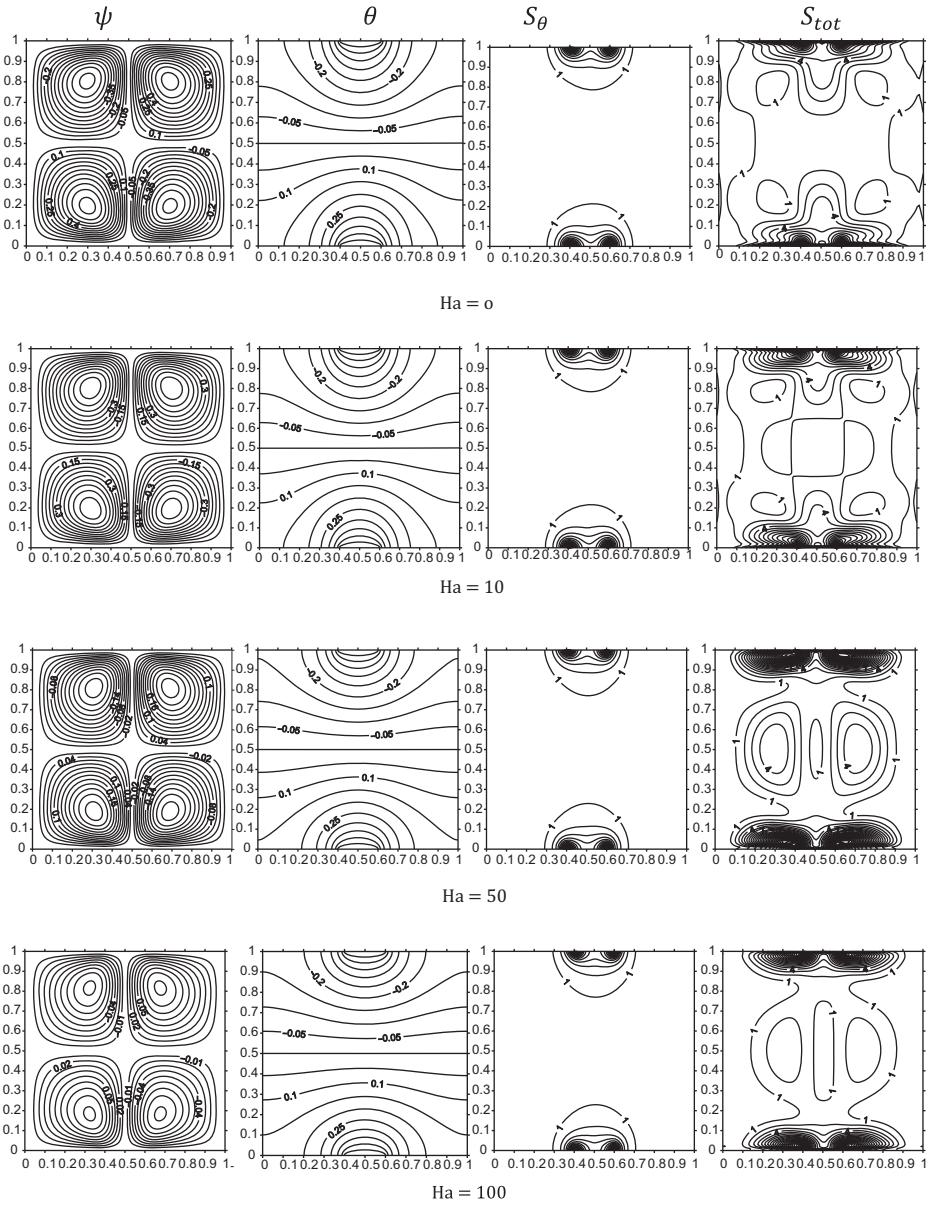

Figure 4.
Contours of streamlines, isotherms, entropy generation due to heat transfer and total entropy generation for different values of Hartmann number *Ha* at $Ra = 10^5$, $Da = 10^{-3}$, $B = 0.2$, $D = 0.5$, $\varepsilon = 10^{-4}$, $\phi = 0.1$

($Ha = 0$), a strong natural convection is obtained. Also, the gradients of temperature and velocities are high, which indicates strong distributions for the entropy generation due to heat transfer and the total entropy generation. As *Ha* increases, a slow motion for the nanofluid is obtained and the contours of the local entropy generation due to heat transfer shrink toward the hot part and the cold part inside the cavity. The contours of the local total

entropy generation are compressed from both sides of the cavity to spread in the middle vertical area in the enclosure. These behaviors are due to the magnetic force which reduces the natural convection.

Figure 5 illustrates the contours of streamlines, isotherms, entropy generation due to heat transfer and total entropy generation for different locations of the heat source D at $Ra = 10^5, Da = 10^{-3}, B = 0.2, Ha = 50, \varepsilon = 10^{-4}, \phi = 0.1$. The results show that the fluid flow takes different profiles for different values of D. At $D = 0.3$, the streamlines represented by two big eddies are formed inside the right-hand side of the enclosure and two small eddies are formed inside the left-hand side of the enclosure. At $D = 0.6$, the fluid flow almost occurs in the left-hand side of the enclosure by forming two big eddies that rotate in the clockwise and counter clockwise directions and stretch in the horizontal direction. Also, there are two small eddies that stretch in the vertical direction. At $D = 0.8$, there are two egg-shaped eddies that can be seen in the enclosure. The isotherm lines and the contours of the entropy generation due to the heat transfer follow the active parts movement. These contours occur at the

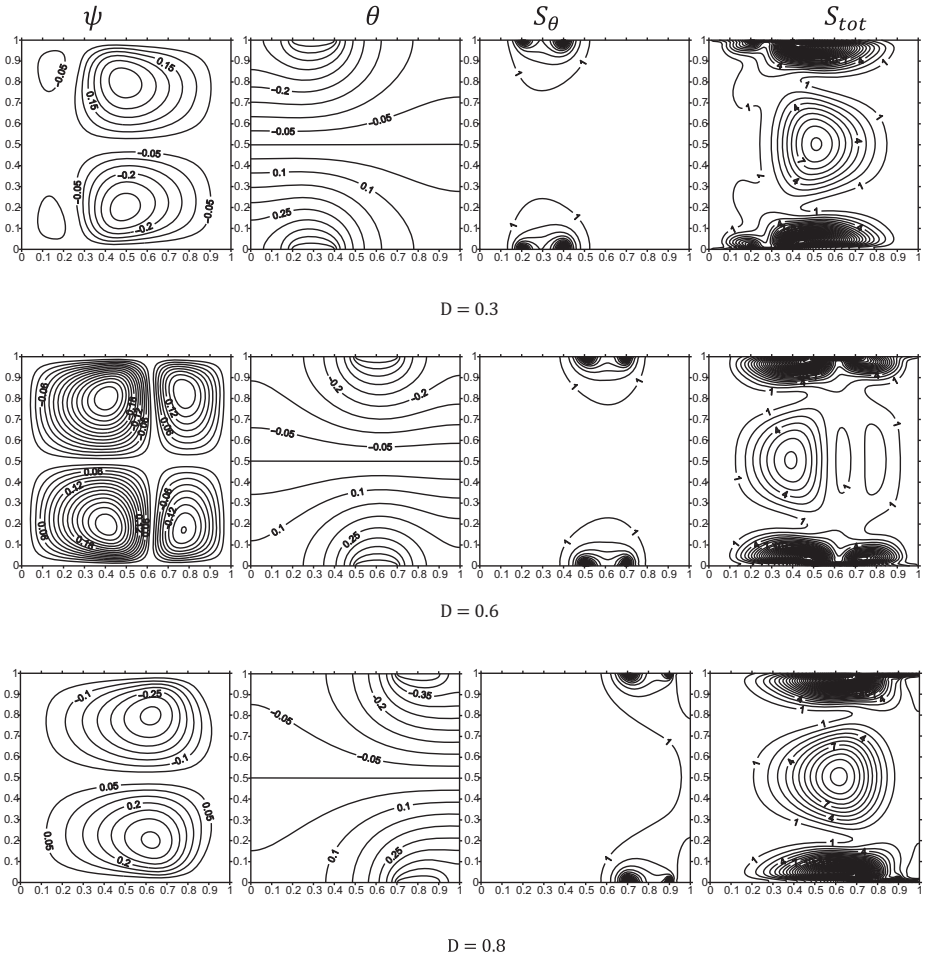

Figure 5. Contours of streamlines, isotherms, entropy generation due to heat transfer and total entropy generation for different locations of the heat source D at $Ra = 10^5, Da = 10^{-3}, B = 0.2, Ha = 50, \varepsilon = 10^{-4}, \phi = 0.1$

left-hand side for $D = 0.3$ and occur at the right-hand side at $D = 0.8$. Moreover, the total entropy generation occurs strongly beside the active parts and in the middle area of the cavity. It can be concluded from this figure that the best location for the active parts is the middle part of the horizontal wall that gives a good natural convection flow.

4.1 Profiles of the entropy generation, local and average Nusselt numbers

Figures 6 and 7 display the profiles of the average total entropy generation and average Bejan number for different values of B and Ha at $Ra = 10^5, Da = 10^{-3}, D = 0.5, \varepsilon = 10^{-4}, \phi = 0.1$. It is found that S_{av} decreases clearly as Hartmann number increases. Unlike the effect of Ha, the increase in $B(B = 0.4)$ results in an increase in S_{av}, whereas more increase in B leads to a decrease in S_{av}. Figure 6 also shows that the minimization of S_{av} occurs at $Ha = 100$ for all values of B. The average Bejan number Be_{av} increases slightly as Ha increases. This behavior is observed for $B = 0.2$, but for $B = 0.4$ and $B = 0.8$, Be_{av} decreases as Ha increases from 0 to 25, whereas as Ha increases from 50 to 100, Be_{av} increases. It can be

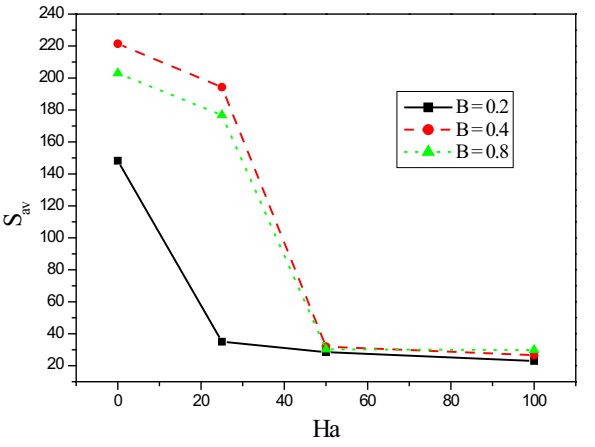

Figure 6.
Profiles of the average total entropy generation for different values of B and Ha at $Ra = 10^5, Da = 10^{-3}, D = 0.5, \varepsilon = 10^{-4}, \phi = 0.1$

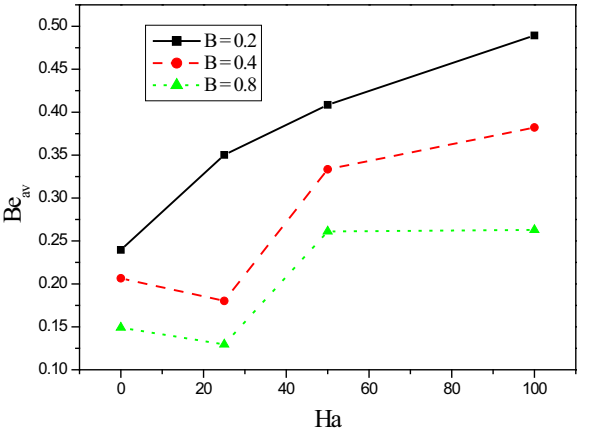

Figure 7.
Profiles of the average Bejan number for different values of B and Ha at $Ra = 10^5, Da = 10^{-3}, D = 0.5, \varepsilon = 10^{-4}, \phi = 0.1$

also seen that for $B = 0.4$ and $B = 0.8$, Be_{av} takes its minimum at $Ha = 25$, whereas for $B = 0.2$, Be_{av} takes its minimum at $Ha = 0$.

Figures 8 and 9 depict the effects of the different locations of the heat source D and variation of the nanoparticle volume fraction ϕ on the profiles of the average total entropy generation Be_{av} and average Bejan number Be_{av} at $Ra = 10^5, Da = 10^{-3}, Ha = 50, B = 0.2, \varepsilon = 10^{-4}$. The average total entropy tends to increase as ϕ increases for all values of D because of the enhancement of the thermal conductivity of the nanofluid as ϕ increases. Also, among all locations of the active parts, $D = 0.6$ was found to be the best location of the active parts and $D = 0.8$ is the bad location. The average Bejan number takes the opposite behavior of S_{av} for all values of ϕ. Moreover, the minimum values of S_{av} are 16.25621, 16.88721 and 15.67379, at $\phi = 0$, for $D = 0.3$, 0.6 and 0.8, respectively. On the contrary, the minimization of Be_{av} occurs at $\phi = 0.1$ for all values of D.

Figures 10 and 11 illustrate the profiles of average total entropy and average Bejan number for different values of Darcy number and viscous dissipation parameter at $Ra = 10^5, Ha = 50, B = 0.2, D = 0.5, \phi = 0.1$. For $Da = 10^{-3}$ and $Da = 10^{-4}$, an increase in ε results in a little increase in S_{av} and Be_{av}, but for $Da = 10^{-5}$, variation of ε does not have any clear

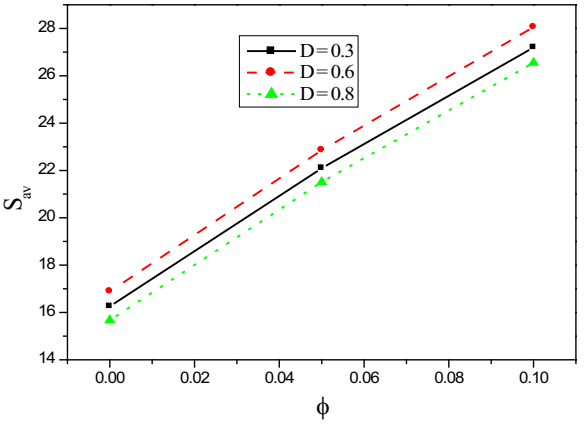

Figure 8.
Profiles of the average total entropy generation for different values of D and ϕ at $Ra = 10^5, Da = 10^{-3}, Ha = 50, B = 0.2, \varepsilon = 10^{-4}$

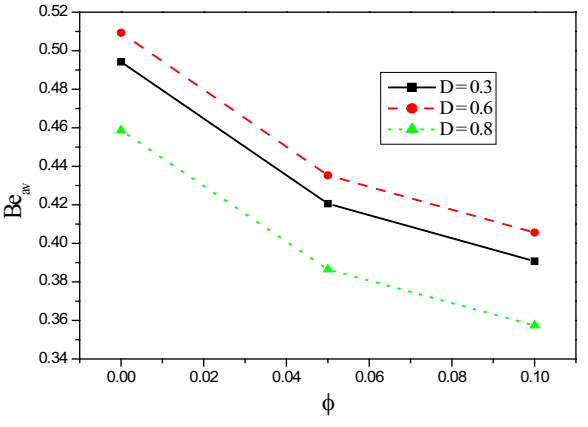

Figure 9.
Profiles of the average Bejan number for different values of D and ϕ at $Ra = 10^5, Da = 10^{-3}, Ha = 50, B = 0.2, \varepsilon = 10^{-4}$

effect on S_{av} and Be_{av}. The minimum values of S_{av} and Be_{av} are 11.07178 and 0.4103309 and occur at $Da = 10^{-5}$ and $Da = 10^{-3}$, respectively.

The effects of active parts of length B, Hartmann number Ha and different locations of the active parts D on the local Nusselt number Nu_s are depicted in Figures 12, 13 and 14. The increase in B leads to a decrease in Nu_s because of the decrease in the temperature gradient. The increase in Ha results in a decrease in the rate of heat transfer. This behavior is observed at the beginning and end of the heated part, whereas at the middle heated part, Nu_s increases as Ha increases. In addition, the best location of the heated part was found to be at $D = 0.3$ that gives a good rate of heat transfer. For all the effects of governing parameter, Nu_s takes its minimum at the center point of the heated part. All these observations are noted in Figures 12, 13 and 14 with a referenced case of $Ra = 10^5$, $Da = 10^{-3}$, $\varepsilon = 10^{-4}$, $\phi = 0.1$.

Figure 15 shows the profiles of the average Nusselt number at the heated part for different values of the heat source length B and Hartmann number Ha at $Ra = 10^5$, $Da = 10^{-3}$, $D = 0.5$, $\varepsilon = 10^{-4}$, $\phi = 0.1$. It is observed that the increase in both B and Ha causes a clear reduction in the average Nusselt number. The physical explanation of this behavior is the

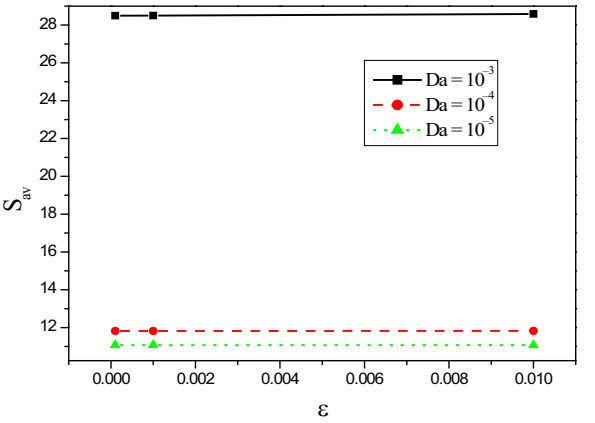

Figure 10.
Profiles of the average total entropy generation for different values of Da and ε at $Ra = 10^5, Ha = 50, B = 0.2, D = 0.5, \phi = 0.1$

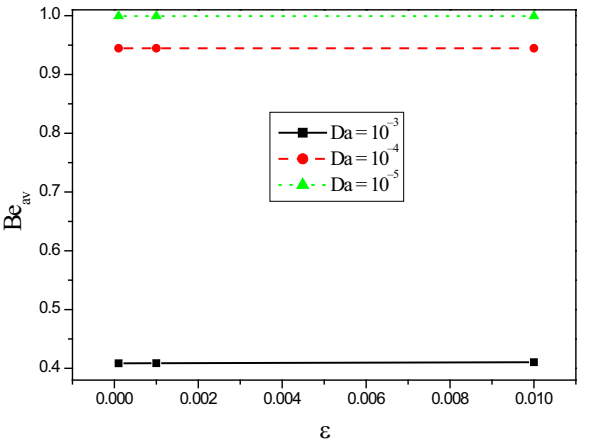

Figure 11.
Profiles of the average Bejan number for different values of Da and ε at $Ra = 10^5, Ha = 50, B = 0.2, D = 0.5, \phi = 0.1$

increase in the heat generation rate which results from the increase in B that decreases the temperature gradient and consequently decreases the average Nusselt number.

5. Conclusions

The effect of viscous dissipation on entropy generation due to MHD natural convection in porous media-filled square cavity with active parts using nanofluid has been investigated in the current paper. The dimensionless partial differential equations governing the problem were solved numerically using the finite volume method. A comparison with previously published results was formulated and was found to be in an excellent agreement. It is found that the increase in length of the heated and cold parts leads to the reduction in natural convection inside the enclosure, which results in a clear decrease in the local total entropy generation. Also, the presence of a magnetic field has negative effects on the local entropy generation due to heat transfer and the local total entropy generation. The increase in Darcy number leads to a decrease in the average total entropy generation and increases the average Bejan number. There is a little increase in average total entropy, and the average Bejan number can be obtained by increasing the viscous dissipation parameter at large values of the Darcy number, whereas at low values of the Darcy number, the viscous dissipation

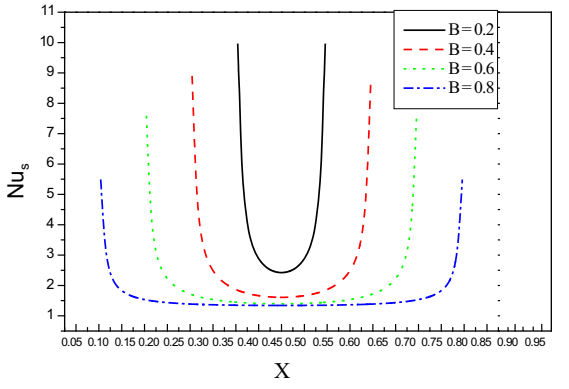

Figure 12.
Profiles of the local Nusselt number for different values of B at $Ra = 10^5$, $Da = 10^{-3}$, $Ha = 50$, $D = 0.5$, $\varepsilon = 10^{-4}$, $\phi = 0.1$

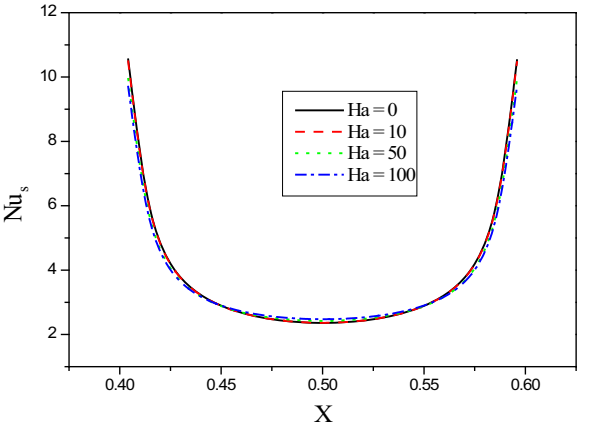

Figure 13.
Profiles of the local Nusselt number for different values of Ha at $Ra = 10^5$, $Da = 10^{-3}$, $B = 0.2$, $D = 0.5$, $\varepsilon = 10^{-4}$, $\phi = 0.1$

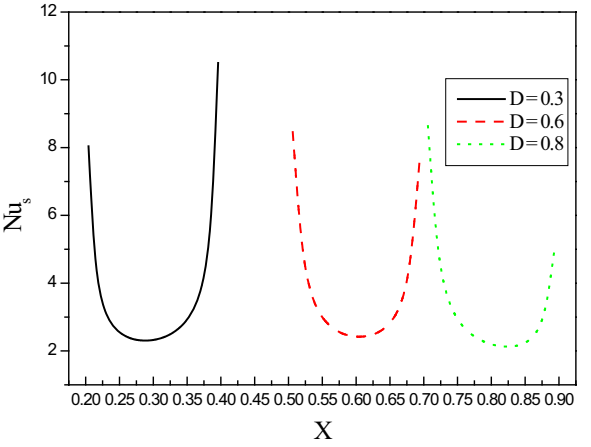

Figure 14.
Profiles of the local Nusselt number for different values of D at $Ra = 10^5$, $Da = 10^{-3}$, $B = 0.2$, $Ha = 50$, $\varepsilon = 10^{-4}$, $\phi = 0.1$

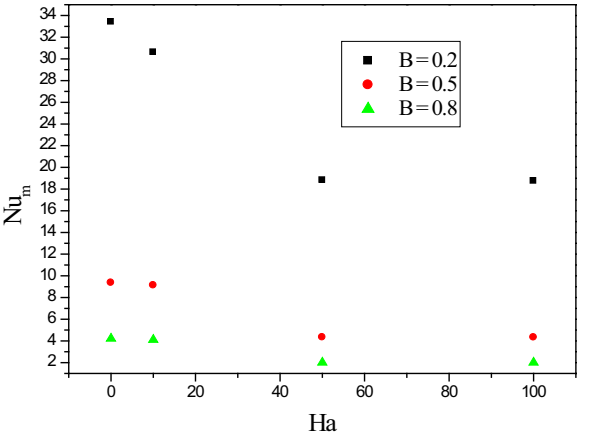

Figure 15.
Profiles of the average Nusselt number for different values of B and Ha at $Ra = 10^5$, $Da = 10^{-3}$, $D = 0.5$, $\varepsilon = 10^{-4}$, $\phi = 0.1$

parameter does not have any clear effects on the average total entropy and average Bejan number. In addition, the rate of heat transfer at the heated part decreases slightly with an increase in the length of the heated and cold parts.

References

Abu-Nada, E. (2011), "Rayleigh-Bénard convection in nanofluids: effect of temperature dependent properties", *International Journal of Thermal Sciences*, Vol. 50, pp. 1720-1730.

Abu-Nada, E., Masoud, Z., Oztop, H. and Campo, A. (2010), "Effect of nanofluid variable properties on natural convection in enclosures", *International Journal of Thermal Sciences*, Vol. 49 No. 3, pp. 479-491.

Ahmed, S.A. (2015), "Mixed convection in thermally anisotropic non-Darcy porous medium in double lid-driven cavity using Bejan's heatlines", *Alexandria Engineering Journal*, available at: http://dx.doi.org/10.1016/j.aej.2015.07.016

AL-Hadhrami, A.K., Elliott, L. and Ingham, D.B. (2003), "A new model for viscous dissipation in porous media across a range of permeability values", *Transport in Porous Media*, Vol. 53, pp. 117-122.

Aminossadati, S.M. and Ghasemi, B. (2011), "Enhanced natural convection in an isosceles triangular enclosure filled with a nanofluid", *Computers & Mathematics with Applications*, Vol. 61, pp. 1739-1753.

Aminossadati, S.M., Raisi, A. and Ghasemi, B. (2011), "Effects of magnetic field on nanofluid forced convection in a partially heated micro channel", *International Journal of Non-Linear Mechanics*, Vol. 46 No. 10, pp. 1373-1382.

Baytas, A.C. (2000), "Entropy generation for natural convection in an inclined porous cavity", *International Journal of Heat and Mass Transfer*, Vol. 43, pp. 2098-2099.

Baytas, A.C. and Pop, I. (1999), "Free convection in oblique enclosures filled with a porous medium", *International Journal of Heat and Mass Transfer*, Vol. 42, pp. 1047-1057.

Beckermann, C., Viskanta, R. and Ramadhyani, S. (1986), "A numerical study of non-Darcian natural convection in a vertical enclosure filled with a porous medium", *Numerical Heat Transfer*, Vol. 10 No. 6, pp. 557-570.

Bejan, A. (1979), "On the boundary layer regime in a vertical enclosure filled with a porous medium", *Letters in Heat and Mass Transfer*, Vol. 6 No. 1, pp. 93-102.

Bejan, A. (1996), *Entropy Generation Minimisation*, CRC Press, Boca Raton, FL.

Brinkman, H.C. (1952), "The viscosity of concentrated suspensions and solution", *Journal of Chemical Physics*, Vol. 20, pp. 571-581.

Cho, S.U.S. (1995), "Enhancing thermal conductivity of fluids with nanoparticles", *ASME Fluids Engineering Division*, Vol. 231, pp. 99-105.

Einstein, A. (1956), *Investigation on the Theory of Brownian Motion*, Dover, NY.

Farooji, V.E., Bajestan, E.E., Niazmand, H. and Wongwises, S. (2012), "Unconfined laminar nanofluid flow and heat transfer around a square cylinder", *International Journal of Heat and Mass Transfer*, Vol. 55, pp. 1475-1485.

Ghasemi, B., Aminossadati, S.M. and Raisi, A. (2011), "Magnetic, field effect on natural convection in a nanofluid-filled square enclosure", *International Journal of Thermal Sciences*, Vol. 50, pp. 1748-1756.

Grosan, T., Revnic, C., Pop, I. and Ingham, D.B. (2009), "Magnetic field and internal heat generation effects on the free convection in a rectangular cavity filled with aporous medium", *International Journal of Heat and Mass Transfer*, Vol. 52, pp. 1525-1533.

Gross, R.J., Bear, M.R. and Hickox, C.E. (1986), "The application of flux-corrected transport (FCT) to high Rayleigh number natural convection in a porous medium", *Proceeding Eighth International Heat Transfer Conference*, *San Francisco, CA*.

Hamad, M.A.A. (2011), "Analytical solution of natural convection flow of a nanofluid overa linearly stretching sheet in the presence of magnetic field", *International Communications in Heat and Mass Transfer*, Vol. 38 No. 4, pp. 487-492.

Hamad, M.A.A. and Pop, I. (2011), "Unsteady MHD free convection flow past a verticalpermeable flat plate in a rotating frame of reference with constant heat source in a nanofluid", *Heat Mass Transfer*, Vol. 47, pp. 1517-1524.

Ilis, G.G., Mobedi, M. and Sunden, B. (2008), "Effect of aspect ratio on entropy generation in a rectangular cavity with differentially heated vertical walls", *International Communications in Heat and Mass Transfer*, Vol. 35, pp. 696-703.

Ingham, D. and Pop, I. (2002), *Transport Phenomena in Porous Media*, Vol. 2, Pergamon Press, Oxford.

Kaluri, R.S. and Basak, T. (2011), "Entropy generation due to natural convection in discretely heated porous square cavities", *Energy*, Vol. 36 No. 8, pp. 5065-5080.

Kandaswamy, P., Sundari, S.M. and Nithyadevi, N. (2008), "Magnetoconvection in an enclosure with partially active vertical walls", *International Journal of Heat and Mass Transfer*, Vol. 51 Nos 7/8, pp. 1946-1954.

Khanafer, K., Vafai, K. and Lightstone, M. (2003), "Buoyancy-driven heat transfer enhancement in a two-dimensional enclosure utilizing nanofluids", *International Journal of Heat and Mass Transfer*, Vol. 46 No. 19, pp. 3639-3653.

Lai, F.C. and Kulacki, F.A. (1988), "Natural convection across a vertical layered porous cavity", *International Journal of Heat and Mass Transfer*, Vol. 31 No. 6, pp. 1247-1260.

Lam, P.A.K. and Prakash, K.A. (2014), "A numerical study on natural convection and entropy generation in a porous enclosure with heat sources", *International Journal of Heat and Mass Transfer*, Vol. 69, pp. 390-407.

Mahmoodi, M. and Hashemi, S.M. (2012), "Numerical study of natural convection of a nanofluid in C-shaped enclosures", *International Journal of Thermal Sciences*, Vol. 55, pp. 76-89.

Mahmoudi, A.H., Shahi, M., Raouf, A. and Ghasemian, A. (2010), "Numerical study of natural convection cooling of horizontal heat source mounted in a square cavity filled with nanofluid", *International Communications in Heat and Mass Transfer*, Vol. 37, pp. 1135-1141.

Mahmoudi, A.H., Pop, I., Shani, M. and Talebi, F. (2013), "MHD natural convection and entropy generation in a trapezoidal enclosure using Cu-water nanofluid", *Computers & Fluids*, Vol. 27, pp. 46-62.

Manole, D.M. and Lage, J.L. (1992), "Numerical benchmark results for natural convection in a porous medium cavity", *ASME Conference, Heat and Mass Transfer in Porous Media, HTD*, Vol. 216, pp. 55-60.

Maxwell, J.C. (1904), *A Treatise on Electricity and Magnetism*, 2nd ed., Oxford University Press, Cambridge, MA.

Moya, S.L., Ramos, E. and Sen, M. (1987), "Numerical study of natural convection in a tilted rectangular porous material", *International Journal of Heat and Mass Transfer*, Vol. 30 No. 4, pp. 741-756.

Nemati, H., Farhadi, M., Sedighi, K., Ashorynejad, H.R. and Fattahi, E. (2012), "Magnetic field effects on natural convection flow of nanofluid in a rectangular cavity using the Lattice Boltzmann model", *Scientia Iranica*, Vol. 19 No. 2, pp. 303-310, doi: 10.1016/j.scient.2012.02.016.

Nield, D.A. and Bejan, A. (2006), *Convection in Porous Media*, Vol. 24, 3rd ed., Springer, Berlin.

Noghrehabadi, A., Pourrajab, R. and Ghalambaz, M. (2012), "Effect of partial slip boundary condition on the flow and heat transfer of nanofluids past stretching sheet prescribed constant wall temperature", *International Journal of Thermal Sciences*, Vol. 54, pp. 253-261.

Noghrehabad, A., Behseresht, A. and Ghalambaz, M. (2013c), "Natural convection of nanofluid over vertical plate embedded in porous medium: prescribed surface heat flux", *Applied Mathematics and Mechanics*, Vol. 34 No. 6, pp. 669-686.

Noghrehabadi, A., Behseresht, A., Ghalambaz, M. and Behseresht, J. (2013b), "Natural-convection flow of nanofluids over vertical cone embedded in non-darcy porous media", *Journal of Thermo Physics and Heat Transfer*, Vol. 27 No. 2, pp. 334-341.

Noghrehabadi, A., Saffarian, M.R., Pourrajab, R. and Ghalambaz, M. (2013a), "Entropy analysis for nanofluid flow over a stretching sheet in the presence of heat generation/absorption and partial slip", *Journal of Mechanical Science and Technology*, Vol. 27 No. 3, pp. 927-937.

Oztop, H.F. and Abu-Nada, E. (2008), "Numerical study of natural convection in partially heated rectangular enclosures filled with nanofluids", *International Journal of Heat and Fluid Flow*, Vol. 29 No. 5, pp. 1326-1336.

Pirmohammadi, M. and Ghassemi, M. (2009), "Effect of magnetic field on convection heat transfer inside a tilted square enclosure", *International Communications in Heat and Mass Transfer*, Vol. 36, pp. 776-780.

Prasad, V. and Kulacki, F.A. (1984), "Convective heat transfer in a rectangular porous cavity effect of aspect ratio on flow structure and heat transfer", *Journal of Heat Transfer*, Vol. 106, pp. 158-165.

Saeid, N.H. (2006), "Natural convection from two thermal sources in a vertical porous layer", *Journal of Heat Transfer*, Vol. 128, pp. 104-109.

Sebdani, S.M., Mahmoodi, M. and Hashemib, S.M. (2012), "Effect of nanofluid variable properties on mixed convection in a square cavity", *International Journal of Thermal Sciences*, Vol. 52, pp. 112-126.

Shohel, M. and Roydon, A. (2002), "Analysis of mixed convection – Radiation interaction in a vertical channel: entropy generation", *Exergy, An International Journal*, Vol. 2 No. 4, pp. 330-339.

Shohel, M. and Sadrul, A.K.M. (2003), "Laminar free convection and entropy generation inside an inclined wavy enclosure", *International Journal of Thermal Sciences*, Vol. 42 No. 1, pp. 1003-1012.

Soleimani, S., Ganji, D., Goji, M., Bararnia, H. and Ghasemi, E. (2011), "Optimal location of a pair heat source-sink in an enclosed square cavity with natural through PSO algorithm", *International Communications in Heat and Mass Transfer*, Vol. 38 No. 10, pp. 652-658.

Sun, Q. and Pop, I. (2011), "Free convection in a triangle cavity filled with a porous medium saturated with nanofluids with flush mounted heater on the wall", *International Journal of Thermal Sciences*, Vol. 50, pp. 2141-2153.

Talebi, F., Mahmoudi, A.H. and Shahi, M. (2010), "Numerical study of mixed convection flows in a square lid-driven cavity utilizing nanofluid", *International Communications in Heat and Mass Transfer*, Vol. 37, pp. 79-90.

Vafai, K. (2005), *Handbook of Porous Media*, Marcel Dekker, New York, NY.

Varol, Y., Oztop, H.F. and Avci, E. (2008), "Natural convection using support vector machines (SVM)in a porous cavity with discrete heat sources", *International Communications in Heat and Mass Transfer*, Vol. 35 No. 8, pp. 928-936.

Walker, K.L. and Homsy, G.M. (1978), "Convection in a porous cavity", *Journal of Fluid Mechanics*, Vol. 87 No. 3, pp. 449-474.

Xuan, Y.M. and Li, Q. (2000), "Heat transfer enhancement of nanofluid", *The International Journal of Heat and Fluid Flow*, Vol. 21, pp. 58-64.

Corresponding author
Ali J. Chamkha can be contacted at: achamkha@yahoo.com